Diffractive amplitude of the absorbed multiperipheral-like model constrained by the inclusive transverse momentum distribution*

Charles B. Chiu, R. J. Gleiser,† and Kuo-Hsiang Wang
Center for Particle Theory, University of Texas, Austin, Texas 78712
(Received 27 August 1973; revised manuscript received 28 May 1974)

With the constraint of the pion inclusive transverse momentum distribution, we deduce a general expression for the diffractive amplitude of the elastic scattering based on the "absorbed multiperipheral-like (MP-like) model" with the independent-emission (IE) parameterization for transverse momentum cutoffs. For comparison, a diffractive amplitude with the multiperipheral (MP) parameterization is also given. For both cases, the diffractive amplitude, together with an added Regge-pole term, gives a reasonable description to pp elastic scattering data for $p_{\rm lab} \gtrsim 10$ GeV/c and $|t| \lesssim 0.8$ GeV^2, where for $p_{\rm lab}$ beyond 100 GeV/c the contribution of the background term is essentially negligible. It predicts that the total cross section ultimately grows like $\sim (\ln s)^2$. Together with the elastic data, the inclusive transverse momentum data are compatible only with the IE case, but not the MP case. This suggests that within the absorbed MP-like model the transverse momenta of the leading particles are essentially not correlated to those of pions.

I. INTRODUCTION

Recently various theoretical ideas[1-8] were discussed in connection with the rise of pp total cross section at the CERN ISR energies.[9] One idea is the application[4] of absorption to the multiperipheral (MP) model, which had been previously suggested in a different context.[10] We have followed up this suggestion and considered absorption for a slightly more general class of models referred to as the multiperipheral-like model.

By MP-like model, we mean those models of multiparticle production which have the following general properties: (1) Particles are produced with a sharp transverse momentum cutoff; (2) the particle multiplicity distribution is Poisson-like, with its average multiplicity $\bar{n} \propto \ln E$, where E is the incident lab energy, $E \approx s/2M$; and (3) the inelastic cross section has a power behavior E^c. Features (1) and (2) are shared by various versions of the MP model[11,12] and those of the independent-emission model[13-15] (IE model). Feature (3) is a prediction of the MP model, although sometimes it is also assumed in the IE model. For the former case, consider for example a simple multi-Regge model, in which there is the emission of M type of species along the MP chain. Ignoring the constraints from the conservation of charge, typically one gets

$$\sigma_{\rm in} \sim E^c ,$$

with

$$c = 2\alpha - 2 + \sum_{j=1}^{M} g_j^2 , \tag{1}$$

where α is the trajectory exchanged and g_j^2 is the coupling of the jth type emitted, with, e.g., the average multiplicity $\bar{n}_j \sim g_j^2 \ln E$.

Empirically feature (1) is well borne out by the data. In theoretical models, this feature is usually implemented through simple factorized cutoff functions. Typically, for an $(n+2)$-particle production amplitude, they are of the form

$$T_{n+2,2} \propto \prod_{i=0}^{n+1} f_i(p_{iT})$$

or (2)

$$T_{n+2,2} \propto \prod_{i=0}^{n} f_i(q_{iT}) ,$$

where the cutoff in the transverse momentum p_{iT} is for the IE model and in momentum transfer $q_{iT} \approx (-t_i)^{1/2}$, for the MP model. So far as the present work is concerned, Eq. (2) is the main expression which distinguishes between the IE case and the MP case. For the experimental support of feature (2), we recall that the pion multiplicity data have been successfully described by the independent-cluster-emission model.[12,14,16] There one finds that the pion multiplicity distribution is essentially Poissonian. For feature (3), if the MP-like model dominates the physical production cross section, the Froissart bound[17] implies $c \leq 0$. So the observed rise of the total cross section cannot be attributed to the asymptotic behavior of the MP-like model.

Instead of looking at the total cross section, the quantity c of Eq. (1) can also be determined independently with the average multiplicity data. In particular, for the π^-, K^-, and $\bar{p}$ average multiplicity data together with the assumption of $\alpha \gtrsim 0.5$, Suzuki[8] estimated that $c > 0$. Although we do not suggest that one should take all the details of his analysis seriously, his work once again reminds

us that there is always a distinct possibility that the MP-like production may have an "apparent violation" of the Froissart bound. Similar to earlier speculations,[4,8] especially that of the QED model[2] of Cheng and Wu, we assume that this violation at the level of MP-like production does indeed occur. However, the Froissart bound is restored in the physical total cross section through further direct-channel mechanisms, such as absorption.

We have analyzed the elastic and the pion inclusive data within the absorbed MP-like model for both the IE case and the MP case of Eq. (2). The simple MP case considered fails to give a simultaneous fit to these data. This confirms previous conclusions.[18-20] On the other hand, the IE case is compatible with these data. The latter case of the absorbed MP-like model is the very model advocated in this paper. On the whole, the main phenomenological support for this IE case is the following:

(1) Within our approach, constrained by some typical pion inclusive distribution, the unabsorbed diffractive amplitude is essentially specified up to normalizations. The available elastic data for $p_{\rm lab} \gtrsim 10$ GeV/c and $|t| \lesssim 0.8$ GeV^2 can be fitted within such a scheme.

(2) It gives a parameter-free prediction[21] to the proton inclusive distribution. This prediction is in crude agreement with the data.

(3) The pion multiplicity distribution for this case is essentially not affected by the absorption. Previously it has been found that a Poisson-like multiplicity distribution in the context of the independent cluster emission model[16] gives a good description to the multiplicity distribution. This can be regarded as another favorable point for the model.

We shall see that for the MP case due to the fact that cutoffs are imposed on the t_i variables, the transverse momentum of each pion emitted is correlated to that of the leading particle. This leads to unwarranted constraints between the elastic and the inclusive data. On the other hand, the "pion–leading-particle correlation" is absent for the IE case. So we extract the following important lesson from our analysis: The data suggest that there is, if at all, only a small fraction of pions having their transverse momenta correlated to those of the leading particles.

The outline of this paper is as follows. In Sec. II, we present a comprehensive discussion on the derivation of the diffractive amplitude for the IE case. In Sec. III, we demonstrate that the diffractive amplitude obtained together with a background Regge-pole amplitude gives an adequate description to the elastic data. In Sec. IV, we study the constraint of the elastic data imposed on the pion inclusive transverse-momentum distribution for the MP case and discuss difficulties involved. Also we compare our present work with the impact-picture model.[2,6] Finally, we give a summary in the same section. For completeness, the asymptotic predictions of elastic scattering, some formulas for the MP case, and the multiplicity distributions of the impact-picture model are given in the Appendixes.

II. THE DIFFRACTIVE AMPLITUDE FOR THE IE CASE

We shall consider exclusively pp collisions. We assume that multiparticle production can be described by two types of processes: simple MP-like production processes and the subsequent interactions among the particles produced. To account for these interactions among the pions and between the pions and nucleons, we adopt the usual cluster-emission picture[12,14,15,22] and crudely describe the final states as NN (or NN^* or N^*N^*) plus n mesons. Here N^* are baryonic excited states and baryonic clusters, and mesons are pions, resonances, and mesonic clusters. For most of our discussions below, it turns out that the identification of the species within either the baryonic or the mesonic classes is not important. For convenience we shall loosely refer to the reactions considered as $pp \to pp + n\pi$, and comment on the effect of resonances or clusters ("clustering effect") at relevant places. The initial- and final-state interactions between the two nucleons will be explicitly accounted for through the rescattering correction or absorption mechanism to be specified below.

In this section we will give a comprehensive discussion on the derivation of the diffractive amplitude only for the IE case and leave the MP case to Appendix B.

A. The unitarity relation and the unabsorbed overlap function H

As usual, we refer the diffractive amplitude to be the asymptotic piece of the elastic amplitude. Presumably its contribution to the total cross section has a power behavior s^0 up to some ln$s$ factor. Also the amplitude is crossing-even, and thus predominantly imaginary. For definiteness, lower-power terms such as $s^{-1/2}$ will not be included in it. We assume that the imaginary part of the diffractive amplitude is given through the

unitarity relation by

$$2\,\mathrm{Im}\,\tilde{T}_{22}(b) = |\mathrm{Im}\,\tilde{T}_{22}(b)|^2 + |\tilde{S}_{22}(b)|^2 \tilde{H}(b)\,,$$

with (3)

$$\tilde{S}_{22}(b) = 1 + i\tilde{T}_{22}(b)\,,$$

where all the quantities in the impact-parameter space are designated by the tilde symbol. We suppress the energy dependence in the arguments, and ignore spin effects. The right-hand side is as usual divided into the contribution of the diffractive part of the elastic amplitude $|\mathrm{Im}\,\tilde{T}_{22}|^2$ and the remaining overlap function, where $\tilde{H}(b)$ is its "unabsorbed" overlap function. We shall specify $\tilde{H}$ below. The absorption factor $|\tilde{S}_{22}(b)|^2$ takes into account both the initial- and final-state interactions between the two nucleons. Here we assume that the interaction between these two nucleons in the presence of pions is essentially the same as for the corresponding elastic scattering. Also, technically speaking, the absorption factor should be evaluated at the relevant impact parameters between the two nucleons throughout the production,[22] which in general differ somewhat from the impact parameter b of the initial state. We shall ignore this difference.

The corresponding quantities of Eq. (3) in t are given by their Fourier-Bessel transform, e.g.,

$$T(t) = \frac{1}{2\pi}\int_{-\infty}^{\infty} d^2b\, e^{i\vec{b}\cdot\vec{\Delta}}\tilde{T}(b)$$

$$= \int_0^{\infty} b\,db\,J_0(b\Delta)\tilde{T}(b) \equiv \langle \tilde{T}(b)\rangle_{\Delta} \qquad (4)$$

and

$$\tilde{T}(b) = \langle T(t)\rangle_b\,, \qquad (5)$$

where $\Delta^2 = -t$. So we have $H(t) = \langle \tilde{H}(b)\rangle_{\Delta}$. The unabsorbed overlap function H at $t=0$ is completely specified by features (2) and (3) of the MP-like model stated in Sec. I. In particular, from the optical theorem,

$$H(t=0) = \frac{1}{2\pi}\sigma_{\mathrm{in}} = \frac{1}{2\pi}\sum_{n=0}^{\infty}\sigma_n = FE^c = FE^c\sum_{n=0}^{\infty}P_n\,, \qquad (6)$$

where F is the over-all normalization constant and P_n the normalized Poisson distribution, with

$$P_n = \left(\frac{E}{E_0}\right)^{-g^2}\frac{[g^2\ln(E/E_0)]^n}{n!}$$

and

$$\sum_n P_n = 1\,, \qquad (7)$$

where E_0 is a scale factor for average multiplicity.

B. From cutoff function $f(p_{iT})$ to $H(t)$

To obtain the t dependence of $H(t)$, we first specify the cutoff function $f(p_{iT})$. Assuming the cutoff functions for pions and protons are all the same, the p_T dependence of the unabsorbed production amplitude ("Born" amplitude) is given by

$$T^B_{n+2,2} \propto \prod_{i=0}^{n+1} f(p_{iT})\,. \qquad (8)$$

For definiteness, we assign the zeroth and the $(n+1)$th particles to be the two protons. It turns out that the eventual predictions of the inclusive p_T distributions of pion and proton based on this simple form are compatible with the data. This gives us *a posteriori* justification for the universality assumption. As we shall see in Sec. II C, for this IE case the effect of absorption on the pion inclusive p_T distribution is negligible. Also the constraint due to the conservation of transverse momentum can be neglected when many particles are present. These two approximations together imply that the cutoff function is given by the square root of the pion inclusive distribu-

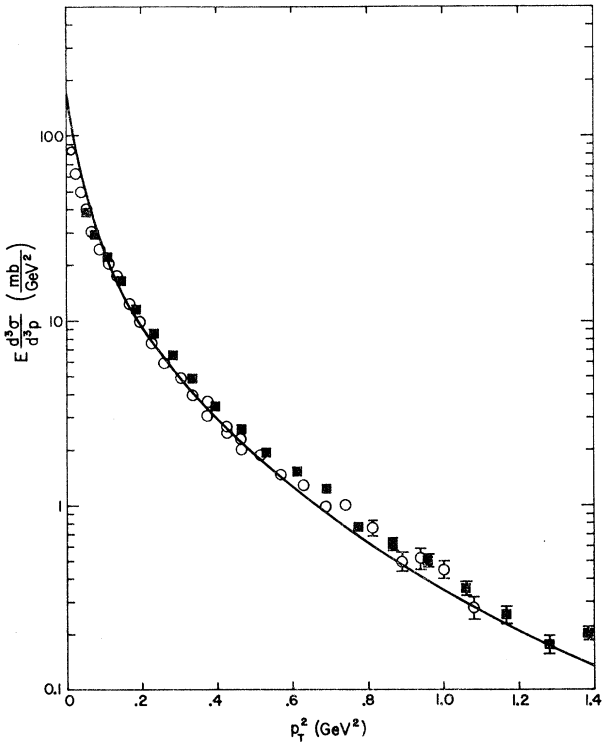

FIG. 1. Comparisons of the pion inclusive distribution between the theoretical cutoff function and the data. Data points with circles are at $\sqrt{s}=30.6$ GeV and $\theta_{\mathrm{c.m.}}=89°$, and those with squares are at $\sqrt{s}=30.4$ and $x=0$. They are from Ref. 23. All distributions are normalized to the 89° data.

tion, which can be directly read off from the data.

Some typical pion p_T-distribution data[23] are illustrated in Fig. 1. A convenient parameterization for this distribution, which also renders a simple analytic form for the overlap function [see Eq. (14) below], is given by

$$f(p_T)=\langle \tilde{f}(b)\rangle_{p_T}$$

with its Fourier-Bessel transform

$$\tilde{f}(b)=\left(\frac{B_1[1+\lambda_1(b^2+B_1^2)^{1/2}]}{(b^2+B_1^2)^{3/2}}\right)^{1/2} \times \exp\{-\tfrac{1}{2}\lambda_1[(b^2+B_1^2)^{1/2}-B_1]\}\ . \tag{9}$$

With[24] $B_1=1.98$ and $\lambda_1=0.32$, it gives the curve in Fig. 1.

The unabsorbed overlap function is in general defined by

$$H(t)=\sum_n \int d\Phi_{n+2}\, T^{B*}_{n+2,2}(\vec{p}_i;\vec{p}_a')\,T^{B}_{n+2,2}(\vec{p}_i;\vec{p}_a) =\sum_n \int d\Phi_{n+2}\, T^{B*}_{n+2,2}(\vec{p}_i+x_i\vec{\Delta};\vec{p}_a) \times T^{B}_{n+2,2}(\vec{p}_i;\vec{p}_a)\,, \tag{10}$$

where the integration is over the phase space of the intermediate state and $x_i\approx 2p_{iL}/\sqrt{s}$, with p_{iL} being the c.m. longitudinal momentum of the ith particle. Also, $\vec{\Delta}=\vec{p}_a'-\vec{p}_a$, where $\vec{p}_a$ and $\vec{p}_a'$ are the initial and final c.m. momenta of one of the protons. In the second step, the rotational invariance of the amplitude has been used. In particular, within the high-energy small-angle approximation, the usual rotation[20] around the y axis with an angle $2\Delta/\sqrt{s}$ is applied.

From Eqs. (8), (9), and (10) we have

$$H(t)=\left\{\prod_{i=0}^{n+1}\int d^2p_{iT} f^*(|\vec{p}_{iT}+x_i\vec{\Delta}|)f(p_{iT})\right\}_{n,L} =\{G_n(t,x_i)\}_{n,L}\,, \tag{11}$$

with[25]

$$G_n(t,x_i)\equiv\prod_{i=0}^{n+1}\int d^2b_i|f(b)|^2 e^{-\vec{b}_i\cdot x_i\vec{\Delta}} =\exp\left(-\sum_{i=0}^{n+1}B_1[(x_i^2\Delta^2+\lambda_1^2)^{1/2}-\lambda_1]\right), \tag{12}$$

where the symbol $\{\cdots\}_{n,L}$ denotes the relevant expression not written out explicitly, which includes the n-dependent normalization factors, an integration over the longitudinal phase space, and a summation over n. After integrating over the longitudinal phase space, we have[26]

$$\{G_n(t,x_i)\}_L\approx FE^c P_n G_n(t,\bar{x}_i)\,, \tag{13}$$

where $\bar{x}_i$ is the rms moment of the x distribution of the ith particle. We make use of the property that for large $\bar{n}_\pi$, the Poisson distribution peaks near its average multiplicity $\bar{n}_\pi$. From Eq. (11) with $G_n(t,\bar{x}_i)\equiv G_n(t)$, we get

$$H(t)\equiv FE^c\sum_n P_n G_n(t)\sim FE^c G(t)\,, \tag{14a}$$

where

$$G(t)=\exp\{-[B_N[(\Delta^2+\lambda_N^2)^{1/2}-\lambda_N] +\bar{n}_\pi B_\pi[(\Delta^2+\lambda_\pi^2)^{1/2}-\lambda_\pi]\}), \tag{14b}$$

and

$$B_N=2\bar{x}_N B_1,\quad \lambda_N=\lambda_1/\bar{x}_N,\quad B_\pi=\bar{x}_\pi B_1\,,$$

and

$$\lambda_\pi=\lambda_1/\bar{x}_\pi\,.$$

Identifying the final-state objects as the "bona fide" protons and pions with λ_1 given earlier, we found typically[27,28] $\lambda_N^2\approx 0.18$ GeV^2 and $\lambda_\pi^2\approx 7$ GeV^2. Since we will be mainly interested in the elastic scattering data for $|t|<1$ GeV^2, the t dependence of the pion term in the exponent of Eq. (14b) is relatively unimportant and can be ignored. Thus we arrive at

$$H(t)\approx FE^c\exp\{-B[(-t+\lambda^2)^{1/2}-\lambda]\}\,, \tag{15}$$

where

$$B=B_N=2\bar{x}_N B_1 \tag{16}$$

and

$$\lambda=\lambda_1/\bar{x}_N\,.$$

Equation (15) remains approximately valid even after the inclusion of the clustering effect.[29]

C. Smallness of pion angular momentum in the IE case

The fact that the pion contribution to the overlap function is relatively unimportant is a crucial feature for the IE case. It is this very feature which together with the absorption will enable us to describe simultaneously the elastic and the inclusive p_T-distribution data. We digress here to look at more closely the meaning of this approximation. Making a Fourier-Bessel transform on Eq. (11), from Eq. (12) we get

$$\tilde{H}(b)=\langle H(t)\rangle_b =\left\{\prod_{i=0}^{n+1}\int d^2b_i|\tilde{f}(b_i)|^2\delta^2\left(\vec{b}-\sum_{i=0}^{n+1}x_i\vec{b}_i\right)\right\}_{n,L}\,. \tag{17}$$

The δ function in the integrand is due to the constraint of the conservation of angular momentum. Clearly the term $x_i\vec{b}_i$ corresponds to the contribu-

tion of the ith particle to the over-all impact parameter $\vec{b}$. The x factor here is also reflected in the coefficient of Δ^2 in Eq. (12). Apparently our approximation of Eq. (15) has its origin from the relative smallness of the c.m. angular momentum associated with pions produced.

Next we come to the inclusive distribution, which will be discussed in detail in Ref. 21. As we shall see,[30] the effect of absorption on the inclusive distribution is, analogous to the case of the overlap function of Eq. (3), also through the absorption factor $\tilde{S}_{22}(b)$, where $\vec{b}=\sum_i x_i\vec{b}_i$. Expanding the absorption factor in x_j, one has

$$\tilde{S}_{22}(b)=\tilde{S}_{22}(b_r)+x_j\vec{b}_j\cdot\hat{b}_r\,\frac{d}{db_r}\,\tilde{S}(b_r)+O(x_j^2), \quad (18)$$

with

$$\vec{b}_r=\vec{b}-x_j\vec{b}_j$$

and

$$\hat{b}_r=\vec{b}_r/b_r\ .$$

Upon integrating over $\vec{b}_j$, due to azimuthal symmetry the term linear in x_j does not contribute to the inclusive cross section. Finally integrating over the longitudinal phase space, one finds that the corresponding correction term[30] in the inclusive distribution is of the order of $\bar{x}_j^2$.

For the pion one has typically[27] $\bar{x}_\pi^2=0.014\ll1$. In turn the absorption factor has a negligible dependence on $\vec{b}_j$. In other words, the original pion inclusive p_T distribution remains essentially unchanged by absorption except for normalization. We have already made use of this feature in Sec. II B. On the other hand, for the proton one has typically[27] $\bar{x}_N^2=0.56$. The dependence of the absorption factor on the corresponding $\vec{b}_j$ cannot be neglected. So the absorption effect has to be taken into account explicitly and the calculation is more involved. We defer the detailed discussions and the comparison with the data to Ref. 21. There the proton inclusive p_T distribution predicted by the model is shown to be in crude agreement with the data.

Finally, let us look at the effect of the absorption on the multiplicity distribution. Similar to our neglect of the pion contribution in the overlap function of Eq. (15), $G_n(t)$ and thus $\tilde{G}_n(b)$ are also approximately independent of n for this IE case. The absorbed $(n+2)$-particle partial cross section is given by

$$\sigma_n^{\rm abs}=\sigma_n\langle\,|\tilde{S}_{22}(b)|^2\tilde{G}_n(b)\rangle_0\,. \quad (19)$$

With the property of $\tilde{G}_n(b)$ mentioned, one finds that the absorbed multiplicity distribution is also approximately the same as that for the unabsorbed case except for the over-all normalization.

D. From the function H to the diffractive amplitude

To obtain the diffractive amplitude from the unitarity relation Eq. (3), we make the approximation that $\tilde{T}_{22}$ is purely imaginary. Solving for the quadratic equation we get

$$\mathrm{Im}\,\tilde{T}_{22}(b)=1-\frac{1}{[1+\tilde{H}(b)]^{1/2}}\ . \quad (20)$$

To ensure that the amplitude $\tilde{T}_{22}(b)$ be even under crossing, we make the usual replacement of E by $Ee^{-i\pi/2}$. Let $\tilde{T}_0(b)$ be the complexified unabsorbed overlap function. Then the complexified elastic amplitude

$$\tilde{T}(b)=i\left(1-\frac{1}{[1-2i\tilde{T}_0(b)]^{1/2}}\right), \quad (21)$$

where

$$\tilde{T}_0(b)=\tfrac{1}{2}i\,F(Ee^{-i\pi/2})^c\,\tilde{G}_c(b) \quad (22)$$

and

$$\tilde{G}_c(b)\equiv\langle G_c(t)\rangle_b \equiv\frac{B_c[1+\lambda(B^2+B_c^2)^{1/2}]}{(b^2+B_c^2)^{3/2}} \times\exp\{-\lambda[(b^2+B_c^2)^{1/2}-B_c]\}\ .$$

The experimental pion average multiplicity is[31]

$$\bar{n}_\pi=g_\pi^2\ln(E/E_0) \approx2.24\ln E-3.44\ . \quad (23)$$

Hence, from Eq. (B5) in Appendix B one has

$$B_c=2\bar{x}_N B \quad \text{for the IE case,}$$
$$=2.24\bar{v}\,B_1(\ln E-\tfrac{1}{2}i\pi)+2\bar{x}_N B_0-4.44\bar{v}\,B_1 \quad \text{for the MP case.} \quad (24)$$

III. COMPARISON WITH pp ELASTIC SCATTERING DATA

As mentioned, our diffractive amplitude is meant to account for only the leading asymptotic behavior of the elastic amplitude. For detailed comparison with elastic data, especially in the low-energy region, a background term has to be added. We choose this to be a proper Regge-pole contribution and write the full elastic amplitude as

$$A(t)=T(t)+R(t), \quad (25)$$

where $T(t)=\langle\tilde{T}(b)\rangle_\Delta$. The relevant Regge trajectories for near forward pp scattering are the ω-ρ and A_2-f^0 trajectories. Their contribution is parameterized as[32]

$$R(t)=[-\beta_+(e^{-i\pi\alpha(t)}+1)+\beta_-(e^{-i\pi\alpha(t)}-1)] \times E^{\alpha(t)-1}e^{at}, \quad (26)$$

where the "±" subscripts designate the even and odd signatures and $\alpha(t)=\frac{1}{2}+t$. In the limit of exchange degeneracy, $\beta_+=\beta_-$. However, because of the oversimplified parameterization, we will not impose this relation on $R(t)$.

With our conventions, the total cross section and the differential cross section are given by

$$\sigma_T=\frac{4\pi}{2.568}\,\mathrm{Im}A(0)$$
$$\approx 4.89\ \mathrm{Im}A(0)\quad(\text{in mb}),\tag{27}$$

and

$$\frac{d\sigma}{dt}=\frac{\pi}{2.568}\,|A(t)|^2$$
$$\approx 1.22|A(t)|^2\quad(\text{in mb/GeV}^2).\tag{28}$$

Here, the conversion factor $\text{mb/GeV}^2=2.568$ has been used. With Eqs. (27) and (28), the present model for both the IE case and the MP case was compared to the pp elastic data[33]: σ_T, $\mathrm{Re}A/\mathrm{Im}A$ at $t=0$, the slope parameters of differential cross section at various t values, and some sample differential cross sections at 12.8, 19.2, and 1500 GeV/c. To further constrain Regge-pole residues, $\bar{p}p$ total-cross-section data[34] are also included. For the $\bar{p}p$ case the factor β_- of the odd-signatured term in Eq. (26) is replaced by $-\beta_-$.

For the IE case, the parameters λ_1 and B_1 are constrained by the pion inclusive data. Only free parameters for the diffractive amplitude are F and c, which are correlated to the energy-dependent normalization of the diffractive contribution. For the MP case, all the parameters are free. This latter case is included mainly for comparison. In our data analysis, no least-squares fit program was used, although sample calculations were made with parameters varied to obtain their optimum values. Typical solutions for both the IE case and MP case are presented in Table I, labeled as solutions I and II, respectively. Notice that in our solution $c>0$. This is a crucial point. All the predictions of the asymptotic behavior discussed below are with positive c.

A. Total cross section

The comparison of solutions I and II with the pp and $\bar{p}p$ total cross-section data[33,34] is shown in Fig. 2. Solid curves are theoretical predictions. Fits are reasonable down to $p_{\mathrm{lab}}=6$ GeV/c. The diffractive contributions alone for both solutions are also shown in the same figure as the dashed curves. Notice that beyond 100 GeV/c this contribution essentially saturates the cross section. The analysis on the ultimate asymptotic behavior of the total cross section is given in Appendix A. With the solutions of Table I,

$$\sigma_T\sim 0.11(\ln E)^2,\quad \text{for the IE case}$$
$$\sim 0.09(\ln E)^2,\quad \text{for the MP case}.\tag{29}$$

The diffractive contribution rises more or less linearly in $\ln E$, at least up to 10^5 GeV/c, although the $(\ln E)^2$ term is expected to dominate eventually.

B. Re/Im ratio

The comparison between the predicted Re/Im ratio of the forward amplitude and the data is shown in Fig. 3. The fit is good for p_{lab} beyond 10 GeV/c. Notice that the diffractive contribution alone gives a positive contribution. As is well known,[32] it is the Regge-pole contribution which is responsible for the substantial negative ratio in the low-energy region. For completeness, the prediction for $\bar{p}p$ is also included in the plot. The ultimate Re/Im ratio can be obtained from Eq. (A10) with the replacement of E by $Ee^{-i\pi/2}$. It gives the well-known form

$$\mathrm{Re}A(0)/\mathrm{Im}A(0)\sim\pi/\ln E\quad\text{for both cases}.\tag{30}$$

From Fig. 3, one sees that the Isabelle energy is still far away from this asymptotic region.

C. Slope parameter

The slope parameter $B(t)$ for the differential cross section is defined by

$$B(t)=\frac{2.44\{\mathrm{Re}A(t)[d\,\mathrm{Re}A(t)/dt]+\mathrm{Im}A(t)[d\,\mathrm{Im}A(t)/dt]\}}{d\sigma/dt}\,.\tag{31}$$

The energy dependence of this parameter at different t is shown in Fig. 4. The theoretical curves are evaluated at $t=0$ and at $t=-0.325$ GeV^2. They are compared with those points in the nearby t region. There is a crude agreement down to $s=20$ GeV^2 or $p_{\mathrm{lab}}=10$ GeV/c.

In Fig. 4, we see that there is a definite difference between the two parameters at $t=0$ and at $t=-0.325$. So far as the present model is concerned, this difference is already present at the unabsorbed level. In particular, replacing B of Eq. (15) by B_c of Eq. (24), the unabsorbed ("Born

TABLE I. Typical solutions.

	Solution I (IE) [a]	Solution II (MP) [b]
Diffractive part:	$F=24.3$ GeV^{-2}	$F=35.0$ GeV^{-2}
	$\lambda=0.43$ GeV	$\lambda_1=0.32$ GeV
	$B_c=2.97$ GeV^{-1}	$B_1=0.087$ GeV^{-1}
	$c=0.09$	$B_0=1.45$ GeV^{-1}
		$c=0.04$
Regge pole:	$\beta_+=9.41$ GeV^{-2}	$\beta_+=9.41$ GeV^{-2}
	$\beta_-=4.34$ GeV^{-2}	$\beta_-=4.34$ GeV^{-2}
	$a=0.7$ GeV^{-2}	$a=1.5$ GeV^{-2}

[a] For the IE case, with (Ref. 27) $\bar{x}_N=0.75$, $\lambda_1=0.32$ GeV, and $B_1=1.98$ GeV^{-1}.

[b] For the MP case, $\bar{x}_N=0.75$ and $\bar{v}=0.77$ were used.

term") slope parameter is

$$B_{\text{Born}}(t)=\frac{\text{Re}\,B_c}{(-t+\lambda^2)^{1/2}}\,. \tag{32}$$

The right-hand side has a square-root branch point at $t=\lambda^2$. Our solutions give $\lambda=0.43\approx 3m_\pi$. So the slope $B_{\text{Born}}(t)$ varies rapidly near $t=0$. Apparently after the absorption and unitarization within the present model, this feature of varying slope still persists, and gives a good description of the data. Ultimately for the absorbed parameter one has from Appendix A,

$$B(0)\sim 0.01(\ln E)^2\ \text{GeV}^{-2},\quad \text{for the IE case}$$
$$\sim 0.007(\ln E)^2\ \text{GeV}^{-2},\quad \text{for the MP case}. \tag{33}$$

D. Differential cross sections

The comparison of our solutions with the differential cross section data[33] at $p_{\text{lab}}=1500$ GeV/c is illustrated in Fig. 5(a). At this energy the diffractive contribution well saturates the elastic amplitude. Thus the curve shown for the IE case is essentially predicted by the pion inclusive p_T distribution, except for the over-all normalization. The well-known "break" in the data is reproduced. As mentioned earlier, within the present model this behavior is closely related to the square-root cut in t.

The differential cross sections at various energies are illustrated in Fig. 5(b). The 12.8- and 19.2-GeV/c data are reasonably well reproduced up to $|t|\approx 0.8$ GeV^2. At 1500 GeV/c, the predicted curve agrees with the data again up to around $|t|\approx 0.7$ to 0.8, although the predicted curve has a dip at $|t|\approx 1.0$ GeV^2, while the data show a dip further out in $|t|$ at $|t|\approx 1.2$ GeV^2.

The predicted differential cross section at

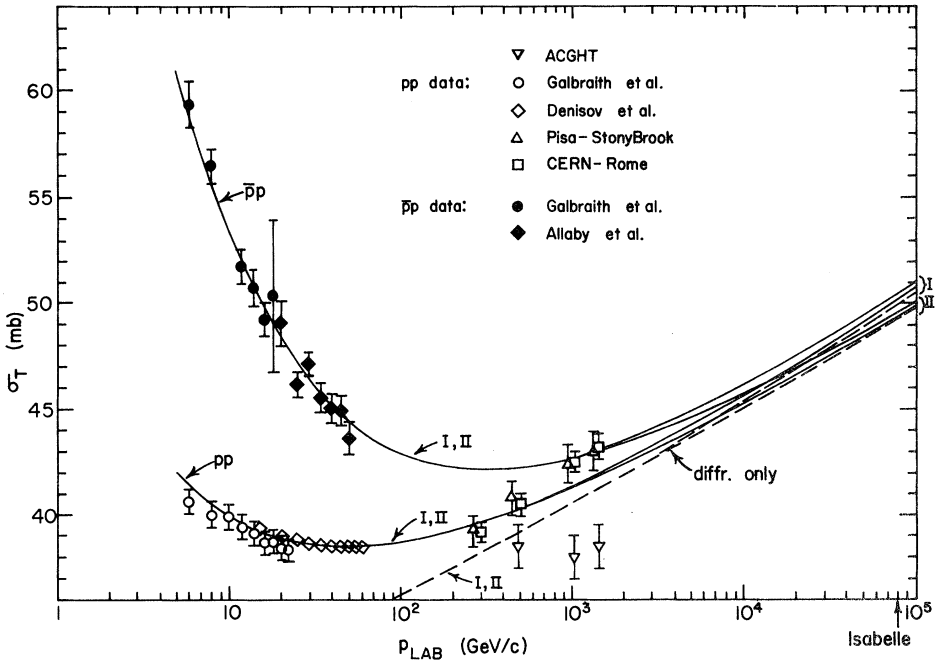

FIG. 2. The pp and $\bar{p}p$ total cross section for incident laboratory energy from 5 to 10^5 GeV/c. Solid curves are model predictions. The dashed curve represents the diffractive term alone. I corresponds to the IE case, and II to the MP case. For data points, see Refs. 33 and 34.

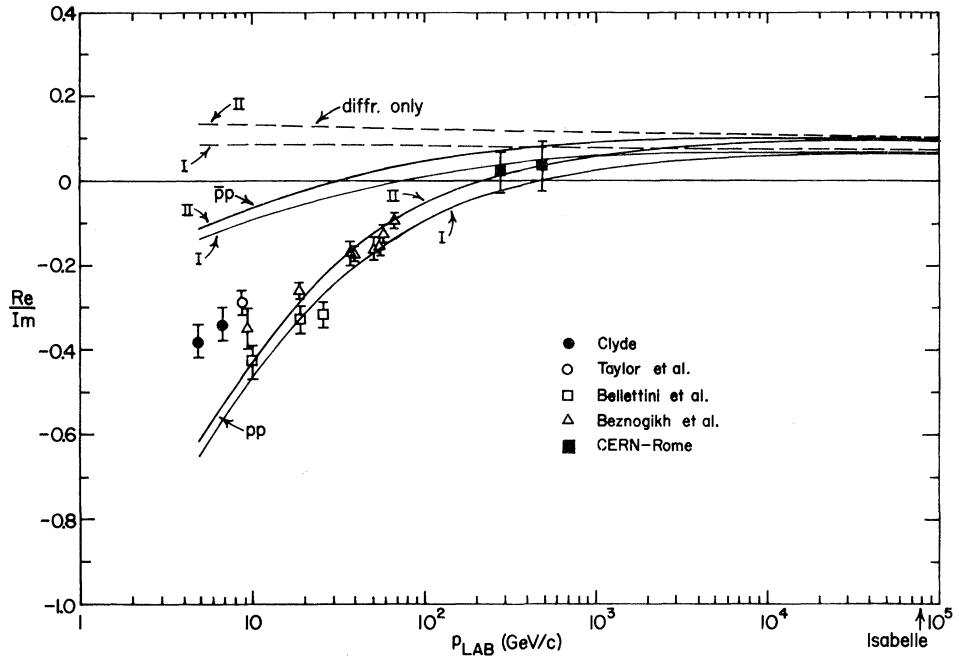

FIG. 3. The ratio of the real part to the imaginary part of the pp and $\bar{p}p$ forward amplitude from 5 to 10^5 GeV/c. Solid curves are model predictions. The dashed curve represents the diffractive contribution alone. I corresponds to the IE-case, and II to the MP case. The data points are for pp only. See Ref. 33 for detail references.

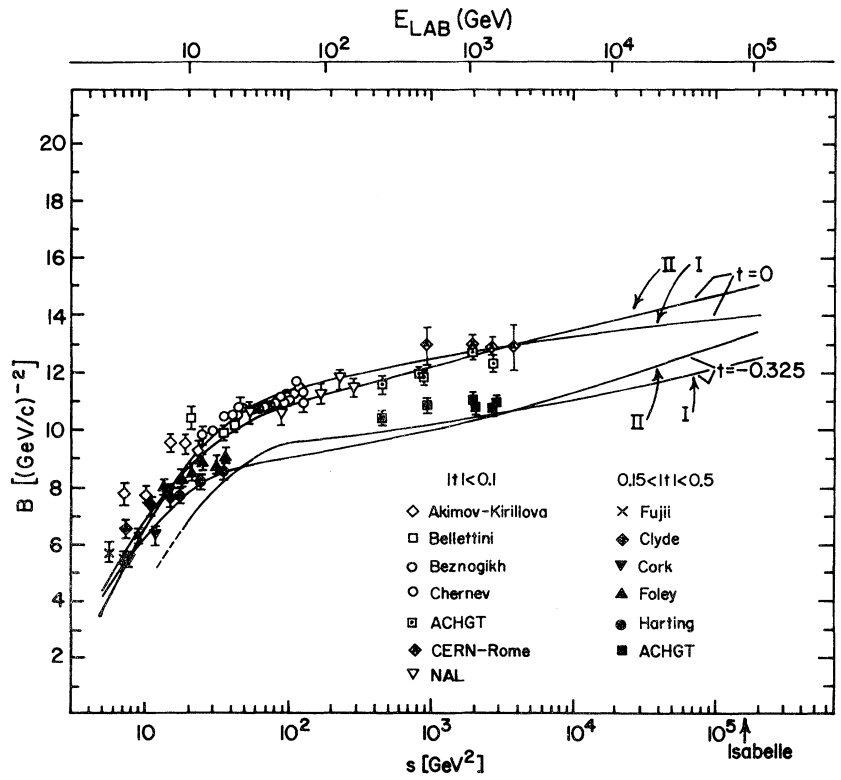

FIG. 4. The slope parameter $B(t)$ for pp differential cross section in the energy region $s=5$ to 2×10^5 GeV^2. Theoretical curves shown are computed at $t=0$ and $t=-0.325$ GeV^2. I corresponds to the IE case, and II to the MP case. The data points as shown are divided into two groups: one with $|t|<0.1$ and the other with $0.15<|t|<0.5$. See Ref. 33.

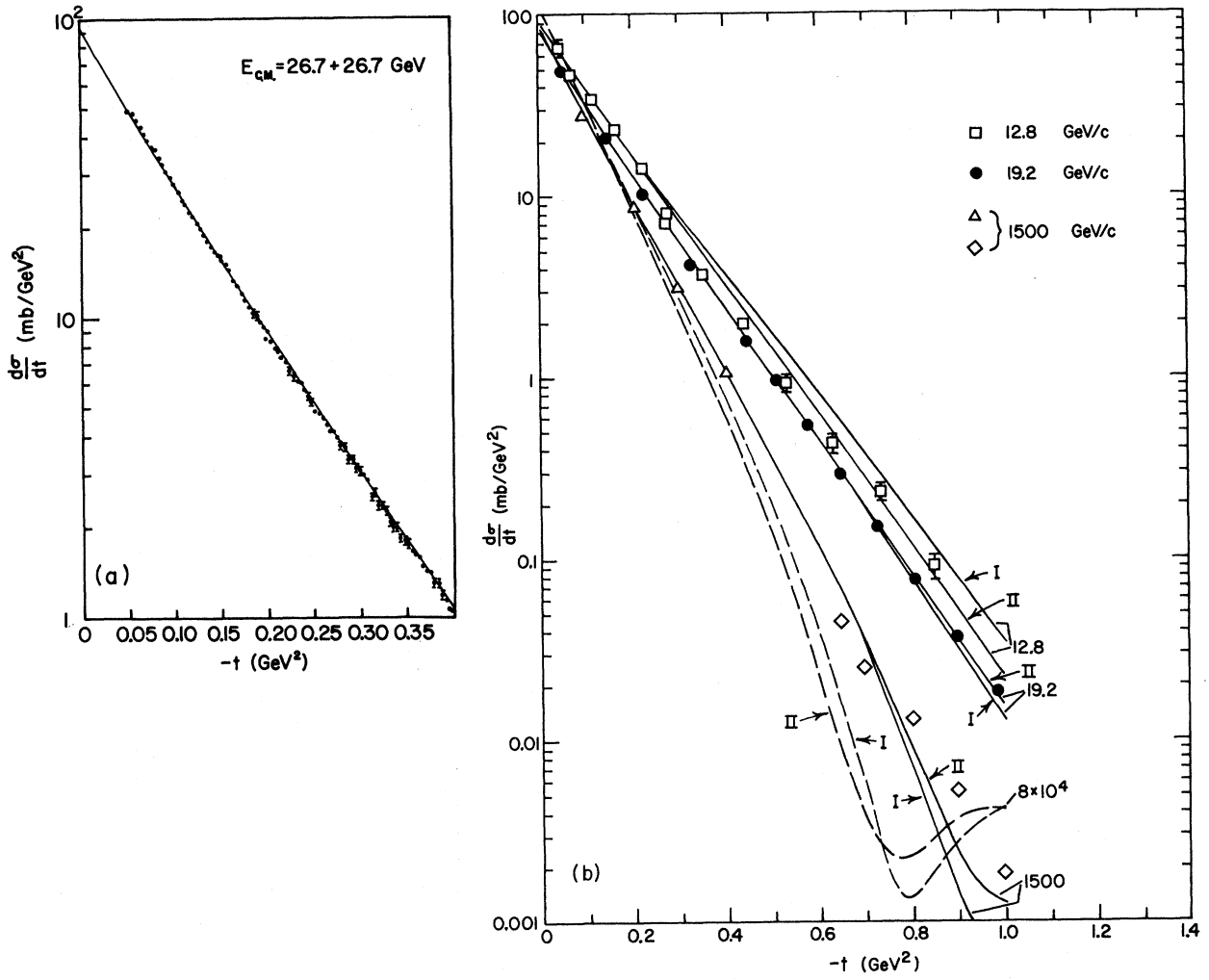

FIG. 5. (a) A comparison between the theoretical curve and the pp differential cross section data at 1500 GeV/c (or $E_{c.m.}$ = 53.4 GeV). Both solutions I and II give essentially the same prediction. For data points see Ref. 33. (b) A comparison between theoretical curves and the differential cross section data at 12.8, 19.2, and 1500 GeV/c. I corresponds to the IE case, and II to the MP case. For data points, see Ref. 33. The prediction at 8×10^4 GeV/c is shown by the dashed curve.

Isabelle energy is also shown in Fig. 5(b). Notice several features in the energy dependence of the predictions:

(1) the rapid shrinkage phenomena,
(2) the inward motion of the dip, and
(3) the rise of the secondary maxima.

These features are quite general and are closely related to the approach of the asymptotic black-disk-like pattern.

IV. DISCUSSION

A. The absorbed MP-like model and the inclusive data

In Sec. II, we have seen that, for the IE case, there is a one-to-one correspondence between the p_T dependence of the cutoff function f and the t dependence of the unabsorbed overlap function H. Our parameters B_1 and λ_1 of Table I for this case are compatible with both the elastic and the pion inclusive data.

For the MP case, with the parameters obtained, the predicted inclusive p_T distribution is grossly different from the data. In particular, constrained by the elastic solution, we found for this case the ratio $\langle p_T^2\rangle_\pi / \langle p_T^2\rangle_N \gg 1$. This disagrees with the data, where this ratio is comparable to unity.[23] It turns out that the qualitative feature of this inconsistency is already present before the absorption. For simplicity, we demonstrate this difficulty for the unabsorbed case with a Gaussian cutoff function. We shall see that our observations

below basically confirm earlier conclusions.[18-20]

In Appendix B, we discuss the MP case in some detail. With the Gaussian cutoff functions, in the form of Eq. (B7)

$$f(p_T) \propto e^{(-b_\pi p_T^2)}$$

and

$$f_0(p_T) \propto e^{(-b_N p_T^2)},$$

from Eq. (B6) the unabsorbed slope parameter is

$$B_{\text{Born}}^{\text{MP}} = 2b_N \bar{x}_N^2 + b_\pi(\bar{n}-1)\bar{v}^2, \tag{34}$$

with $\bar{v}^2$ defined in Eq. (B4). The quantity $\bar{n}$ is the mean of the average multiplicities of pions plus other resonances or clusters. Denote the average number of pions per object emitted to be N_0. Its estimated value at this stage varies from authors to authors. Making the most favorable choice for the MP case, we take one[35] of the largest values proposed, i.e., $N_0 = 3.5$. From Eq. (23), one has

$$\bar{n} = \frac{\bar{n}_\pi}{N_0} \approx g_c^2 \ln(E/E_0) \sim 0.64 \ln E - 0.98. \tag{35}$$

From Eqs. (B9) and (B10), the average values of the squares of the transverse momenta of proton and pion are respectively

$$\langle p_T^2 \rangle_N^B = 1/2b_N$$

and (36)

$$\langle p_T^2 \rangle_\pi^B = 1/b_\pi.$$

From Fig. 4, we obtain the experimental slope parameter at $t=0$,

$$B^{\text{exp}} = 0.39 \ln E + 10.4. \tag{37}$$

With this slope parameter together with Eqs. (35) and (36) and[20] $\bar{v}^2 = 0.6$, we get $b_\pi = 1$ GeV^{-1} and $b_N = 10.3$ GeV^{-1}. In turn, from Eq. (37), one has

$$\langle p_T^2 \rangle_\pi^B / \langle p_T^2 \rangle_N^B \approx 21 \gg 1. \tag{38}$$

Notice that from the point of view of the elastic data, this large ratio stems from the fact that the observed slope of the diffractive peak is relatively large but has a weak energy dependence for the MP case. This large ratio predicts that the proton inclusive p_T distribution should be much sharper than that of the pion. This is contrary to the data, where the two distributions are similar.[23] So with the parameters determined by the elastic data, the MP case does not explain the inclusive p_T distribution. In other words, the simultaneous description of the elastic and the inclusive data cannot be achieved. This is similar to earlier conclusions where, starting with the inclusive p_T data, one shows that the elastic peak cannot be consistently explained.[18-20]

We observe that this failure can be traced to the general structure of the momentum transfer (q_i^2) cutoff of the MP model [see Eq. (2)]. We recall $q_i = \sum_{j=0}^{i} p_j$. Having the cutoff in q_i's, one finds that the transverse momentum of each pion is correlated to that of the leading nucleon. Furthermore, this implies that the contribution of each pion to the t dependence of the unabsorbed overlap function is comparable to that of the nucleon as is clear from Eq. (B6). This feature leads to the discrepancy discussed above.

On the other hand, for the IE case, the transverse momenta of the pions and those of the nucleons are assumed to be uncorrelated. This very feature together with the fact that $\bar{x}_\pi^2 \ll \bar{x}_N^2$ enables us to neglect the pion contribution to the t dependence of the unabsorbed overlap function [see Eqs. (14b) and (15)]. This feature together with absorption leads to a mild energy dependence of the slope parameter, in agreement with the data. We recall the multiperipheral-like productions specified in the beginning of Sec. II are of the type $pp \to NN$ (NN^*, or N^*N^*) plus n mesons. Therefore our analysis here suggests that except for a small fraction of pions from baryonic clusters (they typically are present in the diffractive dissociation events), the momenta of the bulk of the pions are essentially uncorrelated to that of either proton (or more generally either of the leading particles).

B. Comparison of the absorbed MP-like model with the impact-picture model

Our fits to elastic data and the asymptotic predictions are similar to those obtained from the impact-picture model[2,6] (or the eikonal model), although the latter did not consider detailed fits to data below, say, $s \approx 100$ GeV^2, except for the total cross section. In general for $|t| \lesssim 0.8$ GeV^2, where most of the cross section is, apparently the absorbed MP-like models and the eikonal model give a similar description. The elastic data for $|t| \lesssim 1$ GeV^2 appear to be insensitive in distinguishing these models.

We observe that the absorbed MP-like model for the IE case and the eikonal model are based on different multiparticle-production mechanisms. The former corresponds to applying absorption to the MP-like amplitude, while the latter corresponds to the s-channel iterations of the MP-like amplitude. Thus while the predictions of these two models on the elastic process are similar, their predictions on multiparticle production could be different. For the present case, we have shown that there is a simple relation between the pion cutoff function and the corresponding inclusive p_T distribution which is compatible with the data.

A similar comparison for the eikonal case is not available at this stage.

We now look at multiplicity distribution. This distribution, predicted by the present IE case as mentioned earlier, is essentially undisturbed by absorption. We recall that Poisson-like distributions with the inclusion of cluster emissions have been shown[16] to be compatible with the data. This compatibility can now be regarded as another strong point of this model. On the other hand, for the impact-picture model, we assume the usual s-channel iteration structure for multiparticle productions as specified in Appendix C. With this assumption the multiplicity distribution is given by

$$\sigma_n^{\mathrm{IP}} = \frac{[g^2 \ln(E/E_0)]^n}{n!} \sum_{j=0}^{\infty} \frac{j^n}{j!} [(E/E_0)^{-\epsilon^2}]^j \times \langle |\tilde{S}^{\mathrm{IP}}(b)|^2 [\mathrm{Im}\,\tilde{H}(b)]^j \rangle_0 \tag{39}$$

with $\bar{n} \sim E^c/\ln E$. This distribution deviates significantly from a Poisson-like distribution. We have attempted to fit the multiplicity data but have not succeeded in getting reasonable fits, especially for those data beyond 100 GeV/c, even though we did obtain fits to the pion average multiplicity and the correlation parameter, f_2.

C. Summary

The main point extracted from our analysis is that within the present framework, the transverse momenta of pions are essentially uncorrelated to those of the leading protons. We have seen that "the pion-leading-particle correlation" specified by the MP case cannot simultaneously explain the elastic and the inclusive data. On the other hand, this correlation is absent for the present IE case and such simultaneous description has been shown to be possible.

For the IE case, we have exploited the empirical relation, $\bar{x}_\pi^2 \ll \bar{x}_N^2$, which leads to an important feature that the average angular momentum of pions produced is relatively small. This feature subsequently implies the dominance of nucleon contribution to the t dependence of the overlap function and the weak dependence of the absorption factor on the impact parameter of the inclusive pion. This is one of the crucial ingredients which enable us to describe quantitatively the elastic data, the inclusive p_T distributions, and the pion multiplicity distributions.

Some limitations of our model are the following. Within our approach, so far as the longitudinal momentum distribution is concerned, only quantities such as $\bar{x}_\pi^2$ and $\bar{x}_N^2$ are included. Details of the longitudinal exclusive distribution have not been specified. Also we have greatly idealized the final states. Our treatment of this aspect is particularly rudimentary. As the next step, one may ask whether with some proper choice of the exclusive p_L distribution and with the inclusion of a more realistic description of final states, one can achieve an over-all description of pp collisions at high energies.

After the completion of our manuscript, we found that in addition to Ref. 4, absorbed multiperipheral models are also discussed by Finkelstein[36] and by Amati, Caneschi, and Ciafaloni.[37] In the former paper, the simultaneous description of the shrinkage rate of the elastic peak and the inclusive transverse momentum distribution is not examined. In the latter paper, this simultaneous description is discussed in the context of the application of absorption to the triple-Regge formalism.

ACKNOWLEDGMENT

We thank George Sudarshan for encouraging us to look into the ultrahigh-energy physics in connection with the Isabelle project study. This originally instigated our present investigation. One of us (C.B.C.) would like to thank Geoffrey Chew and Frank Henyey for discussions.

APPENDIX A: ASYMPTOTIC FORMULAS

In this appendix, we derive the asymptotic formulas for the total cross section, the inelastic cross section, and the slope parameter at $t=0$. Define the variable $y = D - \lambda(b^2 + B_c^2)^{1/2}$, with $D \equiv \ln[F(Ee^{-i\pi/2})^c \lambda^3 B_c] + \lambda B_c$. For $c>0$, one obtains from Eq. (24)

$$\begin{aligned} D &= c \ln E + O(\ln\ln E), \quad \text{for the IE case} \\ &= (c + \lambda d_0)\ln E + O(\ln\ln E), \quad \text{for the MP case} \end{aligned} \tag{A1}$$

where $d_0 = g_c^2 \bar{v} B_1 = 2.24\,\bar{v} B_1$. From Eqs. (21) and (A1), the elastic amplitude at $t=0$ takes the form

$$T(0) = \langle \tilde{T}(b) \rangle_0 = -\frac{i}{\lambda^2} \int_{D-\lambda B_c}^{-\infty} \left(1 - \frac{1}{(1-2i\tilde{T}_0)^{1/2}}\right)(D-y)\,dy, \tag{A2}$$

where

$$-2i\tilde{T}_0 = (1 + D - y)e^y/(D-y)^3 . \tag{A3}$$

Set $-2i\tilde{T}_0 = 1$ and solve for y. The solution is

$$y_0 = 2\ln\ln E + O(\ln\ln E/\ln E) . \tag{A4}$$

Dividing the integral of Eq. (A2) into two parts,

$$T(0) = T_1 + T_2 , \tag{A5}$$

$$T_1 \equiv -\frac{i}{\lambda^2}\int_{y_0}^{-\infty}\left(1-\frac{1}{(1-2i\tilde{T}_0)^{1/2}}\right)(D-y)dy = \frac{i}{\lambda^2}\int_{D-y_0}^{\infty}\frac{[1+(1+z)z^{-3}e^{-z+D}]^{1/2}-1}{[1+(1+z)z^{-3}e^{-z+D}]^{1/2}}\,z\,dz , \tag{A6}$$

$$T_2 \equiv -\frac{i}{\lambda^2}\int_{D-B_c}^{y_0}\left(1-\frac{1}{(1-2i\tilde{T}_0)^{1/2}}\right)(D-y)dy = \frac{i}{\lambda^2}\int_{\lambda B_c+1}^{D-y_0+1}\left[1-\left(\frac{(z-1)^3z^{-1}e^{z-D-1}}{1+(z-1)^3z^{-1}e^{z-D-1}}\right)^{1/2}\right](z-1)dz . \tag{A7}$$

By expanding the integrands of Eqs. (A6) and (A7) in powers of z, it is straightforward to show

$$T_1 \approx O(D)$$

and

$$T_2 \approx i\left(\frac{D^2}{2\lambda^2}-\frac{B_c^{\,2}}{2}\right)+O(D\ln D) . \tag{A8}$$

From Eq. (A7), the leading term of T_2 and, in turn, that of $T(0)$ have the form

$$T(0)\sim T_2 \sim \frac{i}{\lambda^2}\int_{\lambda B_c+1}^{D-y_0+1}(z-1)dz = i\int_0^{b_{\rm cut}} b\,db , \tag{A9}$$

where $b_{\rm cut}$ is the cutoff impact parameter, which is the solution of the equation, $-2i\tilde{T}_0(b)=1$. Asymptotically $b_{\rm cut}\sim c\ln E/\lambda$ for the IE case, and $b_{\rm cut}\sim[c(c+2\lambda d_0)]^{1/2}\ln E/\lambda$ for the MP case. Thus we arrive at the asymptotic expressions

$$T(0)\sim \frac{i}{2}\frac{c^2}{\lambda^2}(\ln E)^2, \quad \text{for the IE case}$$

$$\sim \frac{i}{2}\frac{c(c+2\lambda d_0)}{\lambda^2}(\ln E)^2, \quad \text{for the MP case} . \tag{A10}$$

From Eq. (27), the corresponding expressions for the total cross sections are:

$$\sigma_T \sim 2.445\frac{c^2}{\lambda^2}(\ln E)^2, \quad \text{for the IE case}$$

$$\sim 2.445\frac{c(c+2\lambda d_0)}{\lambda^2}(\ln E)^2, \quad \text{for the MP case} . \tag{A11}$$

Asymptotically the inelastic cross section is given by

$$\sigma_{\rm in}\sim 4\pi\langle\,|\tilde{S}_{22}(b)|^2\,{\rm Im}\,\tilde{T}_0(b)\rangle_0 . \tag{A12}$$

With similar considerations to those leading to Eq. (A10), after some algebra one finds

$$\sigma_{\rm in}\sim 1.222\frac{c^2}{\lambda^2}(\ln E)^2, \quad \text{for the IE case}$$

$$\sim 1.222\frac{c(c+2\lambda d_0)}{\lambda^2}(\ln E)^2, \quad \text{for the MP case} . \tag{A13}$$

Note that in this asymptotic region $\sigma_{\rm in}\sim\frac{1}{2}\sigma_T$, which is a characteristic feature of black-disk scattering.

With the analogous approach one also finds the slope parameter at $t=0$,

$$B(0)\sim\frac{c^2}{4\lambda^2}(\ln E)^2, \quad \text{for the IE case}$$

$$\sim\frac{c(c+2\lambda d_0)}{4\lambda^2}(\ln E)^2, \quad \text{for the MP case} . \tag{A14}$$

APPENDIX B: FORMULAS FOR THE MULTIPERIPHERAL CASE

1. The unabsorbed overlap function H

For the MP case, the momentum-transfer dependence of the unabsorbed production amplitude is assumed to have the following factorized form:

$$T^B_{n+2,2}\sim\prod_{i=1}^{n-1} f(q_{iT})f_0(q_{0T})f_0(q_{nT}) , \tag{B1}$$

where $q_{iT}^{\,2}\approx -t_i$, $\vec{q}_{iT}=\sum_{j=0}^{i}\vec{p}_{jT}$, and p_{jT} is the transverse momentum of the jth particle. In order to describe the elastic data it is necessary to distinguish the cutoff function of the proton f_0 from that of the pion f. We assume that $f(q_{iT})$ has the same form as $f(p_{iT})$ in Eq. (9) and f_0 is defined with B_1 and λ_1 in f replaced by B_0 and λ_0.

Following a formalism similar to Henyey,[20] we replace the $(n+2)$-particle transverse phase space in Eq. (11) by $\prod_{i=0}^{n} d^2q_{iT}$. This together with Eq. (B1) implies that so far as the transverse part is concerned, the MP case is mathematically identical to an IE case with the replacements

$$n+2\to n+1$$

and

$$p_{iT}\to q_{iT} . \tag{B2}$$

We shall make use of this in later discussion.

From Eqs. (10) and (B1), one has

$$H^{\mathrm{MP}}(t)=\left\{\prod_{i=1}^{n-1}\int d^2q_{iT}f^*(|\vec{q}_{iT}+v_i\vec{\Delta}|)f(q_{iT})\int d^2q_{0T}f_0^*(|\vec{q}_{0T}+v_0\vec{\Delta}|)f_0(q_{0T})\int d^2q_{nT}f_0^*(|\vec{q}_{nT}+v_n\vec{\Delta}|)f_0(q_{nT})\right\}_{n,L}. \tag{B3}$$

Similar to the IE case, one obtains the corresponding overlap function

$$H(t)\approx FE^c\exp\{-2B_0\bar{x}_N[(-t+\lambda_N^2)^{1/2}-\lambda_N]-B_1(\bar{n}_\pi-1)\bar{v}[(-t+\lambda_\pi^2)^{1/2}-\lambda_\pi]\}, \tag{B4}$$

with

$$\lambda_N=\frac{\lambda_0}{\bar{x}_N},\ \lambda_\pi=\frac{\lambda_1}{\bar{v}},\ \text{and}\ \bar{v}^2=\sum_{i=1}^{n-1}\frac{\bar{v}_i^2}{n-1},$$

where as before the bar designates a rms average over the longitudinal distribution. Asymptotically, we assume that $\bar{v}$ does not depend on n. In order to get a similar t dependence to that for the IE case, we take $\lambda_\pi=\lambda_N$ or $\lambda_0/\lambda_1=\bar{x}_N/\bar{v}$. Equation (B4) reduces to Eq. (15), with

$$\begin{aligned}B&=\bar{n}_\pi B_1\bar{v}+2B_0\bar{x}_N-B_1\bar{v}\\&\approx\text{const}+\text{const}\times\ln E\end{aligned} \tag{B5}$$

and

$$\lambda=\lambda_N,$$

where the factor $\ln E$ stems from $\bar{n}_\pi\propto\ln E$. The quantity $\bar{v}$ is bounded: $1\geq\bar{v}\geq\bar{x}_N$. A typical value[20] is $\bar{v}^2=0.6$. We recall the label "π" here actually designates pions, resonances, and clusters. For the discussion below, clustering effect enters explicitly. For clarity we shall replace $\bar{n}_\pi$ by $\bar{n}$, where the latter designates the mean of the average multiplicities of pions, resonances, and clusters.

2. Gaussian cutoff function

With a small-t approximation, the overlap function in Eq. (B4) becomes

$$H(t)\approx FE^c\exp\{[b_N\bar{x}_N^2+\tfrac{1}{2}b_\pi(\bar{n}-1)\bar{v}^2]t\}, \tag{B6}$$

where $b_N=B_0/\lambda_0$, and $b_\pi=B_1/\lambda_1$. The expression in Eq. (B6) can be derived with the Gaussian cutoff functions

$$f_0(q_{iT})\propto e^{-b_Nq_{iT}^2}$$

and

$$f(q_{iT})\propto e^{-b_\pi q_{iT}^2}. \tag{B7}$$

The inclusive p_T distribution is defined by

$$\frac{d^2\sigma}{d^2p_T}\propto\sum_n\int d\Phi'_{n+2}\,T^*_{n+2,2}(p_i;p_a)\,T_{n+2,2}(p_i;p_a), \tag{B8}$$

where $d\Phi'_{n+2}$ is the $(n+2)$-particle phase space with the transverse phase space d^2p_T of the inclusive particle removed. Since $\vec{q}_{0T}=\vec{p}_{0T}$ and $\vec{q}_{nT}=\vec{p}_{n+1T}$, after changing the p's to q's, it follows that

$$\frac{d\sigma}{dp_T^2}\propto\frac{d^2\sigma}{d^2p_T}\propto e^{(-2b_Np_T^2)},\ \text{for the nucleon}. \tag{B9}$$

For the pion, if the inclusive particle is the ith one, again changing p's to q's except for p_{iT}, from Eqs. (B7) and (B8) one has asymptotically

$$\frac{d\sigma}{dp_T^2}\propto\frac{d^2\sigma}{d^2p_T}\propto e^{-b_\pi p_T^2},\ \text{for the pion}. \tag{B10}$$

In general, for a Gaussian case the average transverse momentum squared of pion and nucleon can be read off from Eqs. (B9) and (B10), respectively:

$$\begin{aligned}&\langle p_T^2\rangle_\pi=1/b_\pi\\&\text{and}\\&\langle p_T^2\rangle_N=1/2b_N.\end{aligned} \tag{B11}$$

It is interesting to point out that, if the cutoff functions f for both pion and nucleon were the same ($b_\pi=b_N$), their corresponding average momentum squared would differ by a factor of 2. This can be understood as follows. For the $(n+2)$-particle production, as mentioned, the amplitude in Eq. (B1) can be treated as an independent emission of $(n+1)$ particles with the corresponding transverse momenta q_{iT}. Hence $\langle q_{iT}^2\rangle$ is the same for all i's. For the nucleon, one has $\langle p_T^2\rangle_N=\langle q_{0T}^2\rangle=\langle q_{nT}^2\rangle$. For the pion, one has

$$\begin{aligned}\langle p_T^2\rangle_\pi&=\langle(\vec{q}_{iT}-\vec{q}_{i-1T})^2\rangle\\&=\langle q_{iT}^2\rangle+\langle q_{i-1T}^2\rangle-2\langle\vec{q}_{iT}\cdot\vec{q}_{i-1T}\rangle\\&=2\langle q_{iT}^2\rangle,\end{aligned} \tag{B12}$$

where the term $\langle\vec{q}_{iT}\cdot\vec{q}_{i-1T}\rangle$ vanishes because the q's are uncorrelated. So for $b_\pi=b_N$, one has $\langle p_T^2\rangle_\pi=2\langle p_T^2\rangle_N$.

APPENDIX C: MULTIPLICITY DISTRIBUTIONS IN THE IMPACT-PICTURE MODEL

The impact-picture (IP) model for our discussion here is the same as the eikonal model. For simplicity, we shall only consider the uncomplexified version. Within this model, the inelastic cross section

$$\sigma_{\mathrm{in}}^{\mathrm{IP}}=\langle|\tilde{S}^{\mathrm{IP}}(b)|^2[e^{\tilde{H}(b)}-1]\rangle_0, \tag{C1}$$

where $\tilde{S}^{IP}(b)=\exp[-\frac{1}{2}\tilde{H}(b)]$, and $\tilde{H}(b)$ is given in Eq. (17). We assume that the multiplicity information of the multiparticle production has the usual s-channel iteration structure. In particular, it is specified by the following generating function:

$$\sigma_{in}^{IP}(x)\equiv\sum_n x^n\sigma_n^{IP} =\langle|\tilde{S}^{IP}(b)|^2[e^{\tilde{H}(x,b)}-1]\rangle_0, \quad \text{(C2)}$$

where x keeps track of the number of pions, and

$$\tilde{H}(x,b)=FE^c(E/E_0)^{-g^2}\sum_n\frac{[xg^2\ln(E/E_0)]^n}{n!}\tilde{G}_n(b), \quad \text{(C3)}$$

with $\tilde{G}_n(b)=\langle G_n(t)\rangle_b$.

The average multiplicity is given by

$$f_1^{IP}=\frac{1}{\sigma_{in}^{IP}}\frac{d\sigma_{in}^{IP}(x)}{dx}\bigg|_{x=1} =\frac{1}{\sigma_{in}^{IP}}FE^c(E/E_0)^{-g^2}\sum_{n=1}^{\infty}\frac{[g^2\ln(E/E_0)]^{n+1}}{n!}\times\langle\tilde{G}_{n+1}(b)\rangle_0 =g^2FE^c\ln(E/E_0)/\sigma_{in}^{IP} \sim E^c/(\ln E), \quad \text{(C4)}$$

since $\langle\tilde{G}_{n+1}(b)\rangle_0=1$ and $\sigma_{in}^{IP}\sim(\ln E)^2$. The partial cross section can be obtained by expanding Eq. (C2) in power series of x, which is given in Eq. (39) of the text.

---

*Work supported in part by the USAEC under Contract No. (40-1)3992.

†On leave from Instituto Matematica Astronomia y Fisica, Universidad Nacional de Cordoba, Cordoba, Argentina.

[1]G. F. Chew and D. R. Snider, Phys. Lett. 31B, 75 (1970); F. Zachariasen, review talk given at the NAL conference on Diffractive Phenomena, 1973, Caltech report (unpublished); A. Capella and M.-S. Chen, Phys. Rev. D 8, 2097 (1973); U. P. Sukhatme and J. N. Ng, Nucl. Phys. B 70, 229 (1974).

[2]H. Cheng and T. T. Wu, in *Proceedings of the 1971 International Symposium on Electron and Photon Interactions at High Energies*, edited by N. B. Mistry (Laboratory of Nuclear Studies, Cornell University, Ithaca, N.Y., 1972), p. 148. See also previous papers quoted therein.

[3]S.-J. Chang and T.-M. Yan, Phys. Rev. Lett. 25, 1586 (1970); Phys. Rev. D 4, 537 (1971).

[4]J. Finkelstein and F. Zachariasen, Phys. Lett. 34B, 631 (1971); for the absorbed MP model see also L. Caneschi and A. Schwimmer, Nucl. Phys. B44, 31 (1972).

[5]J. R. Fulco and R. L. Sugar, Phys. Rev. D 4, 1919 (1971); R. Aviv, R. L. Sugar, and R. Blankenbecler, *ibid.* 5, 3252 (1972); S. Auerbach, R. Aviv, R. Sugar, and R. Blankenbecler, *ibid.* 6, 2216 (1972); R. L. Sugar, *ibid.* 8, 1134 (1973).

[6]H. Cheng, J. K. Walker, and T. T. Wu, Phys. Lett. 44B, 97 (1973); 44B, 283 (1973).

[7]D. Sivers and F. von Hippel, Phys. Rev. D 9, 830 (1974); T. K. Gaisser and Chung-I Tan, Phys. Rev. D 8, 3881 (1973).

[8]M. Suzuki, Nucl. Phys. B64, 486 (1973).

[9]S. R. Amendolia *et al.*, Pisa–Stony-Brook collaboration, Phys. Lett. 44B, 119 (1973); U. Amaldi *et al.*, Rome-CERN collaboration, *ibid.* 44B, 112 (1973).

[10]L. Caneschi, Phys. Rev. Lett. 23, 254 (1969).

[11]D. Amati, A. Stanghellini, and S. Fubini, Nuovo Cimento 26, 896 (1962); L. Bertocchi, S. Fubini, and M. Tonin, *ibid.*, 25, 626 (1962); G. F. Chew, M. L. Goldberger, and F. E. Low, Phys. Rev. Lett. 22, 208 (1969); G. F. Chew and A. Pignotti, Phys. Rev. 176, 2112 (1968); C. E. DeTar, Phys. Rev. D 3, 128 (1971); F. Zachariasen, Phys. Rep. 2C, 1 (1971).

[12]H. D. I. Arbarbanel, Phys. Rev. D 6, 2788 (1972); W. R. Frazer, R. D. Peccei, S. S. Pinsky, and C.-I Tan, *ibid.* 7, 2647 (1973); C. J. Hamer, *ibid.* 7, 2723 (1973).

[13]L. Van Hove, Rev. Mod. Phys. 36, 655 (1964); A. Bassetto, M. Toller, and L. Sertorio, Nucl. Phys. B34, 1 (1971); E. H. de Groot and T. W. Ruijgrok, *ibid.* B27, 45 (1971); E. H. de Groot, *ibid.* B48, 295 (1972); D. Sivers and G. H. Thomas, Phys. Rev. D 6, 1961 (1972); D. K. Campbell, *ibid.* 6, 2658 (1972).

[14]C. P. Wang, Phys. Rev. 180, 1463 (1969); B. R. Webber, Nucl. Phys. B43, 541 (1972); E. L. Berger, D. Horn, and G. H. Thomas, Phys. Rev. D 7, 1412 (1973); S. Pokorski and L. Van Hove, Acta Phys. Pol. B 5, 229 (1974).

[15]R. P. Feynman, *Photon-Hadron Interactions* (W. A. Benjamin, New York, 1972), Lectures 52–54.

[16]C. B. Chiu and K.-H. Wang, Phys. Rev. D 8, 2929 (1973).

[17]M. Froissart, Phys. Rev. 123, 1053 (1961).

[18]R. C. Hwa, Phys. Rev. D 8, 1331 (1973).

[19]C. J. Hamer and R. F. Peierls, Phys. Rev. D 8, 1358 (1973).

[20]F. S. Henyey, Phys. Lett. 45B, 363 (1973); 469 (1973).

[21]C. B. Chiu and K.-H. Wang, University of Texas, CPT Report No. 224 (unpublished).

[22]C. B. Chiu and K.-H. Wang, CPT Report No. 186 (unpublished).

[23]Multiparticle production data:

(a) Pion inclusive longitudinal momentum distribution. The 102- and 205-GeV/c data are given in Figs. 3 and 5 of J. Whitmore, in *Experiments on High Energy Particle Collisions—1973*, proceedings of the international conference on new results from experiments on high energy particle collisions, Vanderbilt University, 1973, edited by Robert S. Panvini (A.I.P., New York, 1973), pp. 18 and 20.

(b) Pion inclusive transverse momentum distribution. ISR data: At $\sqrt{s}=30.4$ GeV and $x=0$, see M. Banner *et al.*, Saclay-Strasbourg Collaboration, Phys. Lett. 41B, 547 (1972); at $\sqrt{s}=30.6$ and $\theta_{c.m.}=89°$, see B. Alper *et al.*, Phys. Lett. 47B, 75 (1973).

(c) Proton inclusive longitudinal momentum distri-

bution. M. Antinucci *et al.*, in *Experiments on High Energy Particle Collisions—1973,* proceedings of the international conference on new results from experiments on high energy particle collisions, Vanderbilt University, 1973, edited by Robert S. Panvini [see (a) above], p. 244, Fig. 6.

(d) Proton inclusive transverse momentum distribution. F. T. Dao *et al.*, in *Experiments on High Energy Particle Collisions—1973,* proceedings of the international conference on new results from experiments on high energy particle collisions, Vanderbilt University, 1973, edited by Robert S. Panvini [see (a) above], p. 54, Fig. 11.

(e) The multiplicity distributions. 102 GeV/c: J. W. Chapman *et al.*, Phys. Rev. Lett. 29, 1686 (1972); 205 GeV/c: G. Charlton *et al.*, *ibid.* 29, 515 (1972); 303 GeV/c: F. T. Dao *et al.*, *ibid.* 29, 1627 (1972).

(f) The average multiplicity at 103 GeV/c is taken from Chapman *et al.*, in *Experiments on High Energy Particles—1973,* proceedings of the international conference on new results from experiments on high energy particle collisions, Vanderbilt University, 1973, edited by Robert S. Panvini [see (a) above], together with the assumption of charge independence (i.e., $n_\pi = 3n_-$). It is 6.6.

[24]The parameters B_1 and λ_1 enter in both the t dependence of the elastic amplitude and the pion inclusive p_T distribution. The values quoted here were originally obtained from fits to the elastic data as described in Sec. III, although the predicted pion inclusive distribution based on these values as shown in Fig. 1 is also quite satisfactory. We observe that the conclusions of the present paper are not sensitive to the details of the mathematical form of the cutoff function assumed. For instance, we have also reproduced both the elastic and the inclusive data within the IE case with the cutoff function as superposition of Gaussian functions.

[25]*Tables of Integral Transforms* (Bateman Manuscript Project), edited by A. Erdélyi (McGraw-Hill, New York, 1954), Vol. II, p. 9, Sec. 8.2, Eq. (23).

[26]The approximation involved in Eq. (13) is as follows. Since the most interesting region is at small t, we expand both sides of Eq. (13) in powers of t, and find that the coefficients of t^0 and t^1 terms are identical. For the t^2 terms, the difference consists of the coefficients with the factor, either $(\langle x_i^2 x_j^2\rangle - \langle x_i^2\rangle\langle x_j^2\rangle)$ or $(\langle x_i^4\rangle - \langle x_i^2\rangle^2)$, where the $\langle\cdots\rangle$ symbol here denotes the averaging over the normalized x distributions, e.g., $\langle x_i^2\rangle = \bar{x}_i^2$. For those cases where i or j stands for pion, due to the fact that the pion x distribution peaks near $x=0$, these coefficients are very small (see Ref. 27). For the two nucleons, we assume that the correlation between them is not very strong and neglect the corresponding terms. A similar approximation is also involved in dropping terms with higher powers of t.

[27]Some typical values are $\bar{x}_\pi^2 = 0.014$ and $\bar{x}_N^2 = 0.56$. We explain these estimations here. We have analyzed the normalized pion inclusive x distribution data at a typical energy, e.g., 102 GeV/c [Ref. 23(a)]. The first moment and the rms moment of the x distribution with $x>0$, are found to be respectively $\bar{x}_\pi = 0.085$ and $\bar{x}_\pi = 0.12$. For the proton, we will explain in Ref. 28 that it is difficult to extract the relevant value of $\bar{x}_N$ directly from the corresponding proton data. We obtain this value from the pion information together with the constraint of the conservation of energy: $2\tilde{x}_N + \bar{n}_\pi \tilde{x}_\pi = 2$, where $\tilde{x}_N$ is the first moment of the proton x distribution and $\bar{n}_\pi$ is the pion average multiplicity. At this energy one has $\bar{n}_\pi \sim 6.6$ (Ref. 23) and thus $\tilde{x}_N = 0.72$. From the general shape of the proton x distribution one expects $\bar{x}_N > \tilde{x}_N$. As explained in Ref. 24, our parameters λ_N and B_N were originally determined from the elastic data. According to Eq. (14b), $\lambda_1 = \bar{x}_N \lambda_N$ and $B_1 = B_N/2\bar{x}_N$. We have found that the eventual inclusive distributions predicted are not too sensitive to specific choice of $\bar{x}_N$ within the range: $0.72 < \bar{x}_N < 1$, although there is a tendency that the fits to the pion and proton p_T distribution are improved slightly for larger values of $\bar{x}_N$. We made a conservative estimate and chose $\bar{x}_N = 0.75$. Furthermore, the pion x distributions at 102 and 205 GeV/c [Ref. 23(a)] indicate that the distribution $x d\sigma/dx$ is approximately independent of energy. So the quantity $\bar{n}_\pi \bar{x}_\pi$, and in turn $\bar{x}_N$, could be roughly constant.

[28]We did not extract the relevant quantity $\bar{x}_N$ from the proton x distribution directly. The reason is as follows. Within our model, the proton multiplicity is two. On the other hand, there appears to be a central plateau at high energy in the proton x distribution [Ref. 23(c)] which will give rise to a ln$s$ increase in the average multiplicity. This plateau could be due to the $\bar{N}N$ production, not included explicitly in the present model. To extract the pertinent $\bar{x}_N$ value from the proton data, one has to first remove the central-region contribution. This turns out to be difficult due to the fact that the value of $\bar{x}_N$ so obtained is very sensitive to the specific subtraction assumed. We thus choose to estimate its value from the pion information as described in Ref. 27.

[29]We observe that with the inclusion of clusters the corresponding rms value $\bar{x}$ is in general larger than $\bar{x}_\pi$, while the cluster average multiplicity $\bar{n}$ decreases compared to $\bar{n}_\pi$. These two effects have the tendency to compensate each other.

[30]To be more precise, it is shown in Ref. 22 that the inclusive distribution can be expressed in the form

$$\frac{d\sigma}{dp_T^2} \propto \left\{ \int \prod_i d^2b_i\, d^2b_j'\, \tilde{S}_{22}^*\left(\left|\sum_i x_i \vec{b}_i\right|\right) \times \tilde{H}^{(n)}(\vec{b}_i; p_T; \vec{b}_i') \times \tilde{S}_{22}\left(\left|\sum_{i\neq j} x_i \vec{b}_i + x_j \vec{b}_j'\right|\right)\right\}_{n,L},$$

where p_T is the transverse momentum of the inclusive jth particle. The inclusive overlap function $\tilde{H}(\vec{b}_i; p_T; \vec{b}_i')$ has the following properties: It does not have the x_j dependence and it is invariant under the simultaneous sign change of $\vec{b}_j$ and $\vec{b}_j'$. From these properties and Eq. (18), one can show that the correction term to the p_T dependence of the inclusive distribution due to absorption is of $O(x_j^2)$.

[31]The present negative-pion average multiplicity data can be represented with $f_1^- = -1.15 + 0.74 \ln E$ (see Ref. 16, for example). This in turn leads to Eq. (23).

[32]For a review on the parameterization of Regge-pole contribution and related topics, see, for example, C. B. Chiu, Annu. Rev. Nucl. Sci. 22, 255 (1972).

[33]The pp data:

(a) σ_T. 6–22 GeV/c: W. Galbraith *et al.*, Phys. Rev. 138, B913 (1965); 15–60 GeV/c: S. P. Denisov *et al.*, Phys. Lett. 36B, 415 (1971); 300–1500 GeV/c: See

Ref. 9, and Giacomelli's review in *Proceedings of the XVI International Conference on High Energy Physics, Chicago-Batavia, Ill., 1972,* edited by J. D. Jackson and A. Roberts (NAL, Batavia, Ill., 1973), Vol. 3, p. 266 (hereafter referred to as paper G).

(b) Re/Im. 5,7 GeV/c: A. R. Clyde, Ph.D. thesis, Univ. of California, Berkeley, report, 1966 (unpublished); 8 GeV/c: A. E. Taylor *et al.*, Phys. Lett. 14, 54 (1965); 10, 19, and 26 GeV/c: G. Bellettini *et al.*, *ibid.* 14, 164 (1965); 9–70 GeV/c: G. G. Benzogikh *et al.*, *ibid.* 39B, 411 (1972); 300–500 GeV/c: U. Amaldi *et al.*, *ibid.* 43B, 231 (1973). See also paper G, p. 286.

(c) Slope parameter. Data are from Fig. 14 of paper G, p. 288.

(d) *Differential cross section.* 12.8 GeV/c: K. J. Foley *et al.*, Phys. Rev. Lett. 11, 425 (1963); 19.2 GeV/*(d)* J. V. Allaby *et al.*, Phys. Lett. 28, 67 (1968); 1500 GeV/c (ISR 26.7+26.7 GeV/c): The $|t| \lesssim 0.4$ data are from G. Barbiellini *et al.*, *ibid.* 39B, 663 (1972); the $|t| > 0.6$ GeV^2 data are by the Aachen-CERN-Harvard-Geneva-Torino collaboration, taken from Fig. 2 of the first paper in Ref. 5.

[34]The $\bar{p}p$ total cross section data: 6–8 GeV/c: W. Galbraith *et al.*, Phys. Rev. 138, B913 (1965); 20–65 GeV/c: J. V. Allaby *et al.*, Phys. Lett. 30B, 500 (1969).

[35]T. Ludlam *et al.*, Yale University Report No. Yale C00-3075-61, 1973 (unpublished).

[36]J. Finkelstein, Phys. Rev. D 8, 4176 (1973).

[37]D. Amati, L. Caneschi, and M. Ciafaloni, Nucl. Phys. B62, 173 (1973).